J. Fluid Mech. (1992), *vol.* 237, *pp.* 671–687
Printed in Great Britain

Internal temperature distributions of droplets vaporizing in high-temperature convective flows

By SHWIN-CHUNG WONG AND AR-CHENG LIN
Department of Power Mechanical Engineering, National Tsing Hua University, Hsinchu, Taiwan, ROC

(Received 5 April 1991 and in revised form 22 October 1991)

Transient internal temperature distributions of vaporizing droplets have been carefully measured, using fine thermocouples at 1 atm. and 1000 K. Droplet diameters are fixed at 2000 ± 50 μm with Reynolds numbers being 17, 60 or 100. Fuels tested are JP-10, *n*-decane and JP-10 thickened with polystyrene. The effects of Reynolds number and liquid viscosity on internal temperature distribution and heating mechanism have been examined. Experimental results indicate that liquid viscosity or circulation intensity strongly affects the temperature distribution and heating mechanism. In contrast, the temperature distributions associated with the three different Reynolds numbers have shown little difference for both low- and high-viscosity cases. For the low-viscosity JP-10 droplets at Reynolds numbers up to 100, where the vortex model of Sirignano and coworkers (Prakash & Sirignano 1978; Tong & Sirignano 1983) has been claimed to be applicable, the vortex model appears qualitatively correct but quantitatively inaccurate. Physical reasons for the deviation have been discussed. Solutions of the full Navier–Stokes equations appear to accord better with the experimental temperature distributions. Circulative heat transport decreases progressively as liquid viscosity increases. A semi-empirical effective conductivity model for high-viscosity cases yields a very good simulation of the experimental temperature distributions at all the Reynolds numbers when proper effective conductivity factors are chosen. A discussion on internal droplet dynamics and heating mechanisms in physical terms has been provided.

1. Introduction

Studies on droplet dynamics in convective flows have attracted great academic and engineering interest in recent decades. In a variety of applications such as spray combustion, spray drying, etc., the evaporation rate and droplet trajectory are essentially related to internal droplet dynamics. In these applications considerable velocity and temperature differences usually exist between the vaporizing droplets and ambient gases. Viscous shear resulting from the velocity differences between the gas and liquid induces circulation within the droplet. The circulation would enhance internal transport of momentum, heat, and species (for multicomponent droplets). The enhanced internal transport rates would in turn affect the heating, evaporation rate and hydrodynamic drag associated with the droplet. Importance in understanding internal dynamics and heating mechanisms, especially for vaporizing multicomponent droplets, has been clearly discussed in Law (1982).

Experiments yielding temporally-resolved velocity or temperature fields inside the droplet have long been needed in gaining a full understanding of the internal dynamics and heating mechanisms. Such measurements, however, have been

unavailable owing to considerable experimental difficulties. Past experimental results were limited to either global characteristics, such as evaporation rate and drag coefficient (Renksizbulut & Yuen 1983), or surface characteristics, such as surface velocity (LeClair *et al.* 1972). Details in such complex processes have mostly been found through analytical investigation.

Batchelor (1956) analysed isothermal internal droplet motion at large Reynolds numbers (Re). He suggested that a thin viscous boundary layer exists near the droplet surfaces, with the motion in the droplet core essentially being the inviscid Hill vortex. LeClair *et al.* (1972) and Rivkind, Ryskin & Fishbein (1976) subsequently substantiated this with numerical solutions of the Navier–Stokes equations in both the liquid and the gas phase. The internal streamline patterns were also found to closely resemble those of the Hill vortex for a wide range of Re and ratios of fluid viscosities and densities, while the vortex intensity varied significantly with respect to the variation of these parameters.

For the more complex problem of vaporizing droplets, Sirignano and coworkers (Prakash & Sirignano 1978; Tong & Sirignano 1983; Abramzon & Sirignano 1989) treated the internal liquid flow fields using a boundary-layer approach. They assumed for large Reynolds numbers that: (i) the internal streamlines conform with those of the inviscid Hill vortex; (ii) the internal velocity field may be approximated by the Hill vortex solution; and (iii) the temperature distribution along a streamline is isothermal as Re is sufficiently large. They suggested, through order-of-magnitude analysis, that Re of $O(100)$ would be sufficiently large for the third assumption to be valid. It will be shown in this paper that the latter two assumptions are questionable and their calculations appear qualitatively correct but over-predictive in internal temperature variation. Nevertheless, these works have made considerable advancements in that the essential physics of mass and momentum transport could be determined analytically rather than empirically. Ayyaswamy and coworkers (Gogos & Ayyaswamy 1988; Ayyaswamy, Sadhal & Huang 1989) recently developed a perturbation analysis to solve the Navier–Stokes equations for both the liquid and the gas phase. This technique was applied to evaporation or condensation of moving droplets at small $Re\,(<1)$ or intermediate $Re\,(\approx O(100))$ (Ayyaswamy *et al.* 1989). Circulation intensity was found to be important in actual evaluation of the extent of transport. However, the internal droplet dynamics and heating mechanisms were not discussed in their works. More detailed descriptions of the internal droplet dynamics and heating mechanisms of vaporizing droplets have been rendered by Dwyer, Sanders and coworkers (Dwyer & Sanders 1984; Patnaik *et al.* 1986; Dwyer 1989). By solving the Navier–Stokes equations in both phases, temporally-resolved internal streamline, vorticity, and isotherm patterns were obtained for a range of Re up to $O(100)$ (Patnaik *et al.* 1986). Isotherm patterns for Re of $O(100)$, based on their results, significantly differed from the streamline patterns, while the latter still closely resembled those of the Hill vortex. Droplet core temperatures were still significantly lower than surface temperatures, although they were considerably elevated owing to circulative heat transport. Closed isotherms, during the heating period, only existed in a small region near the vortex centre. These internal temperature distribution results differ from those of Sirignano and coworkers' vortex model. The differences have been attributed to the breakdown of the large Re assumption as Re decreases below $O(100)$ with the liquid evaporating away (Dwyer 1989). It will be shown in this paper that Dwyer and coworkers' results accord better with the present experimental data and the differences are actually because Sirignano and coworkers seemed to overestimate the internal circulative motion at

Re of $O(100)$. Sirignano and coworkers' large-Re vortex model, as a result, can be valid only for even larger Re (say, $O(1000)$). No information concerning the effects of internal circulation intensity or liquid viscosity was provided in Dwyer & Sanders (1984), Patnaik *et al.* (1986), and Dwyer (1989). Dwyer, Sanders and coworkers have provided exciting results as far as internal droplet dynamics and heating mechanisms are concerned, although the development of their models is still incomplete (Dwyer 1989).

This study provides the first quantitative measurements of temporally resolved internal temperature distributions for droplets vaporizing in a high-temperature environment at intermediate $Re(O(10)$–$O(100))$. The effects of Reynolds number and liquid viscosity on internal temperature distribution and heating mechanism have been examined. These data not only render insights into the internal droplet dynamics and heating mechanisms of droplets vaporizing in convective hot flows but also provide valuable experimental data for the evaluation of model reliability.

2. Experimental

2.1. *Experimental methods*

Internal temperature distributions of droplets at intermediate Reynolds numbers ($Re = U_\infty d/\nu_g$) were measured using fine thermocouples within suspended droplets. With the droplets rapidly exposed to 1000 K gas flows, internal temperature variations with respect to time were recorded at various radial positions. Temporally-resolved temperature distributions, using this method, can be obtained without resorting to complex techniques (Winter 1990, *23rd Symp. (Intl) on Combust.* Poster Session). Besides, relatively large Re can be obtained without much difficulty, in comparison with the small Re (usually < 1) associated with the existing free-falling droplet methods. Temperature measurement of internal temperature distribution of free-falling droplets at intermediate or large Re is otherwise rather difficult, if not impossible. The only drawback of the present method is the unavoidable interference from the thermocouple wires and the suspender. This problem has been minimized and should be immaterial. There is a detailed discussion of this interference in §2.2.

The arrangement of the droplet and thermocouples is shown in figure 1. The droplet ($d_0 = 2000 \pm 50$ μm) was suspended on a suspender, which is a ceramic shell attached to a 100 μm diameter glass filament. This thin shell-shaped suspender should cause minimum interference to the internal liquid motion. One or three fine chromel–alumel thermocouples (with 25 μm wire diameter and approximately 70 μm bead diameter) were used to yield rapid response (ca. 5 ms) and negligible interference on internal liquid motion. The resolution of the temperature acquisition system (Data Precision 6100) was 1 K. The heat conducted into the droplet through thermocouple wires were estimated to be insignificant (§2.2).

Hot gas (1000 ± 30 K) for heating droplets was supplied either by a flat-flame burner or an electrical heater. The flat-flame burner, similar to the one used by Wong & Turns (1987), was fuelled with CO, O_2 and N_2. A ceramic honeycomb was placed on the top of the burner chimney to cool the post-flame gas to 1000 K. The oxygen concentration of the gas was 10.4%. The gas velocity, measured using a laser-Doppler velocimeter (one-component, Aerometrics), was 1 m/s. The initial Reynolds number (Re_0) was estimated to be 17. For larger Reynolds numbers the electrical heater (Wong, Lin & Chi 1991), was used. Two test conditions ($Re_0 = 60$ and 100) were then set up. Gas temperatures in both cases were determined using 70 μm bead-diameter chromel–alumel thermocouples.

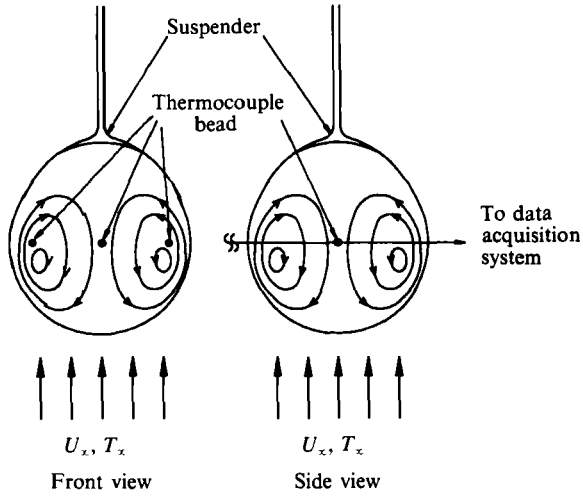

FIGURE 1. Arrangement for measurement of internal droplet temperature.

	JP-10	JP-10/5 wt % polystyrene	JP-10/10 wt % polystyrene
k	0.0795 (W/mk)†	0.082	0.0844
C_p	1943.5 (J/kgK)	1938.2	1932.9
ρ	870.5 (kg/m^3)	882.5	894.5
ν	1.15 (cSt)	7.2	25.0

† according to Antaki & Williams (1987).

TABLE 1. Liquid properties at 100 °C
(approximate average of the boiling point and room temperature)

During a test, the droplet was rapidly exposed to the hot gas by quickly withdrawing a protective shield. Voltage outputs of the thermocouples during the droplet lifetime were stored in a data acquisition system. Droplet diameter variation was simultaneously recorded using a video recorder (Sony V900). The droplets were nearly spherical, according to video records. Effective droplet diameters were evaluated by approximating the particles as ellipsoids. Internal droplet temperature distributions were measured along a horizontal line which passed through the droplet centre by carefully adjusting the horizontal positions of the thermocouple bead(s) prior to the test.

Fuels tested were n-decane, JP-10 (exo-tetrahydrodicyclopentadiene) and JP-10 thickened with polystyrene. Some physical properties of these fuels are listed in table 1.

2.2. *Suspender and thermocouple interferences*

As far as the suspender is concerned, little disturbance on the internal liquid motion is anticipated. This is because the thin shell-like suspender stays near the droplet surface and is located around the rear stagnation point where liquid motion is stagnant.

Disturbance on internal motion from the thermocouple wires is also anticipated to be insignificant. Consider the thermocouple wire as a cylinder subjected to liquid flow. The maximum liquid velocity occurs at the droplet surface and is approximately

$U_\infty/(\rho_l \mu_l/\rho_g \mu_g)^{\frac{1}{3}}$ (equation (1)). The maximum liquid velocity for the present cases is less than 0.2 m/s. The maximum Reynolds number is then

$$Re_l = \frac{U_s d_{tc}}{\nu_l} < \frac{0.2 \text{ m/s} \times 25 \times 10^{-6} \text{ m}}{1.15 \times 10^{-6} \text{ m}^2/\text{s}} = 4.34,$$

which is far less than the critical Reynolds number (about 60) when separation occurs (Schlichting 1979).

The upper limit of the fraction of the heat conducted into the droplet through the thermocouple wires and the suspender is estimated as

$$\frac{\dot{q}_{tc}}{\dot{q}} \approx \frac{\frac{1}{2} n \pi (d_{tc})^2 k_{tc} + \frac{1}{4} \pi (d_{gl})^2 k_{gl}}{\pi d^2 k_g},$$

where $\dot{q}_{tc}$ and $\dot{q}$ are respectively the heat transfer rates through the thermocouples and the droplet surface; n is the number of thermocouples; k_{tc}, k_{gl} and k_g are respectively the conductivity coefficients of the thermocouple, the glass filament and the gas; d_{tc}, d_{gl} and d are respectively the thermocouple wire diameter, glass filament diameter and the droplet diameter. Let $n = 3$, $d_{tc} = 25$ μm, $d_{gl} = 100$ μm, $d = 2000$ μm, $k_{tc} = 25$ W/m K, $k_{gl} = 5.85$ W/m K, and $k_g = 0.067$ W/m K, then $\dot{q}_{tc}/\dot{q} \approx 0.14$. The actual fraction should be acceptably small since this value corresponds to the upper limit.

Another possible temperature measurement error arose from the heating of the thermocouple bead by the heat conducted through the higher-conductivity thermocouple wire. The heating might cause overmeasurements of internal liquid temperature, which can be easily examined based on experimental $T-t$ data. If the heating was negligible, the droplet temperature would reach the steady wet-bulb temperature as long as the bead was wetted. With this heating present, the temperature readings would gradually increase instead of remaining at the wet-bulb temperature. According to experimental results, except when the bead was located at the outer region of the droplet, the temperature readings generally remained near the wet-bulb temperature without a significant increase before the bead was exposed to the ambient gas. Representative results can be found in figure 2.

An event occurred in temperature measurements at large r/R. The bead at large r/R would finally be exposed to the gas since the droplet gradually shrank owing to evaporation. Owing to surface tension the liquid usually stuck to the bead for a while, with exposure being somewhat delayed. This event provided more information concerning droplet surface temperature, although the droplet shape was temporarily distorted.

In summary, most experimental results should be reliable except for slight errors probably existing at large r/R.

3. Results

Internal temperature distributions during the heating period were measured for droplets of JP-10, n-decane and JP-10 thickened with polystyrene at $T_\infty = 1000$ K and atmospheric pressure. Initial droplet diameters were fixed at 2000 ± 50 μm. Initial Reynolds numbers were 17, 60 and 100. Theoretical calculations based on the conduction limit model (CLM), the vortex model (VM), and the effective conductivity model (ECM) were performed, when appropriate, for comparison (for details of these models, see the Appendix).

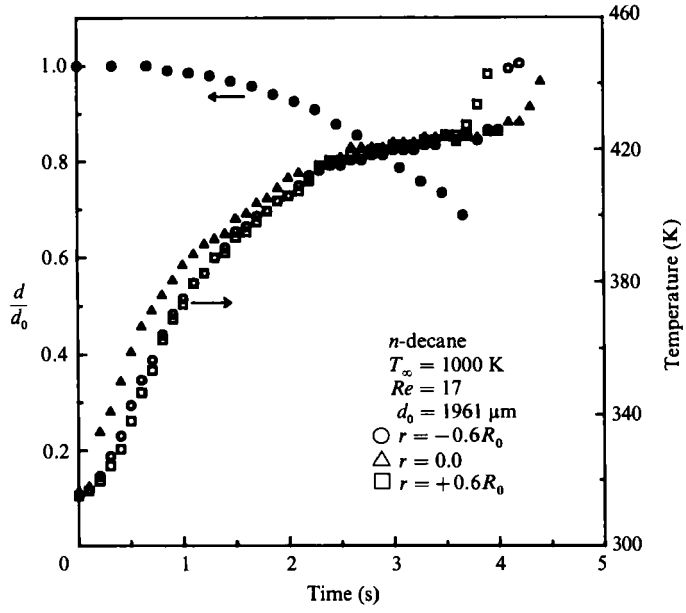

FIGURE 2. Representative experimental results of droplets temperature versus time ($Re_0 = 17$).

Figure 2 presents a set of representative results of internal temperature measurements at $Re_0 = 17$ using three thermocouples. One thermocouple, in this case, was located at the droplet centre with the other two being symmetrically at each side with $r/R_0 = 0.60$. The droplet centre temperature appearing higher with the two symmetrically-located off-centred thermocouples yielding nearly the same temperatures indicates: axisymmetric internal circulation indeed existed to enhance heat transport; and the results of the present experimental method should be reliable. All three temperatures rose to the wet-bulb temperature (ca. 420 K) at $t = 3$ s. Also shown is the droplet diameter history. Little reduction in diameter and hence in Reynolds number was observed during the early period of the heating stage. Reduction in Reynolds number during the first 2 s was less than 10%.

Temporally resolved internal temperature distributions were obtained by repeating tests with thermocouple positions carefully varied (figure 3(*a*) for JP-10 and figure 3(*b*) for *n*-decane). Owing to axisymmetry, data obtained at both sides were integrated in these figures. The closed symbols represent the results from one-thermocouple measurements while the three-thermocouple measurements are represented by open symbols. No differences were observed between one- and three-thermocouple measurements. No mutual interference existing between the three thermocouples is indicated as a result. The minimum temperatures in both figures occur around $r/R = 0.6$–0.7. The temperatures of the droplet core are somewhat higher than the minimum values; they are, however, significantly lower than the temperatures near the droplet surface. This temperature distribution pattern clearly indicates the existence of internal circulation, which enhances heat transport from the droplet surface to the interior.

Experiments were managed at up to $Re_0 = 100$, where the VM has claimed to be applicable ($Re \approx O(100)$). Larger Reynolds numbers were not achieved because the droplet no longer stayed nearly spherically on the suspender. Theoretical calculations based on VM (Tong & Sirignano 1983) were carried out for comparison in this case

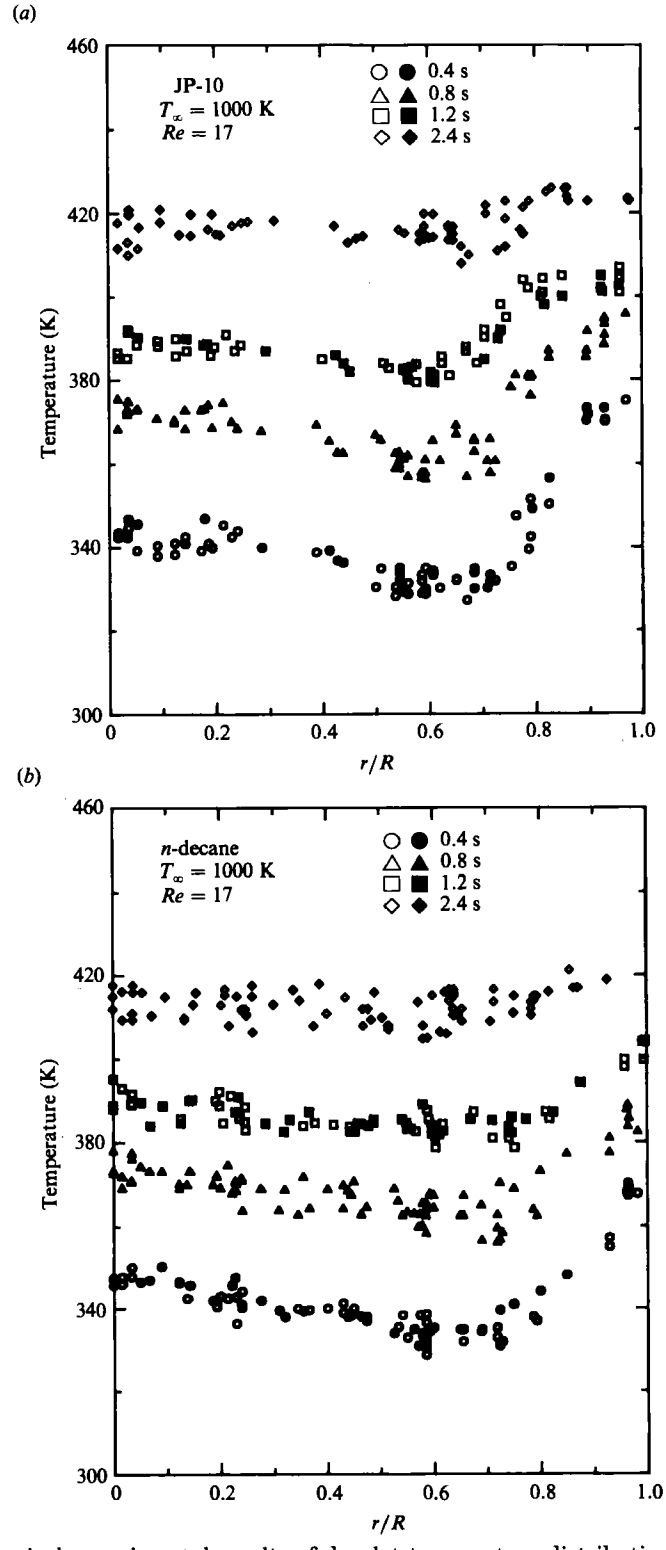

FIGURE 3. Typical experimental results of droplet temperature distribution with respect to time (Re_0 = 17), (*a*) JP-10 droplet (*b*) *n*-decane droplet.

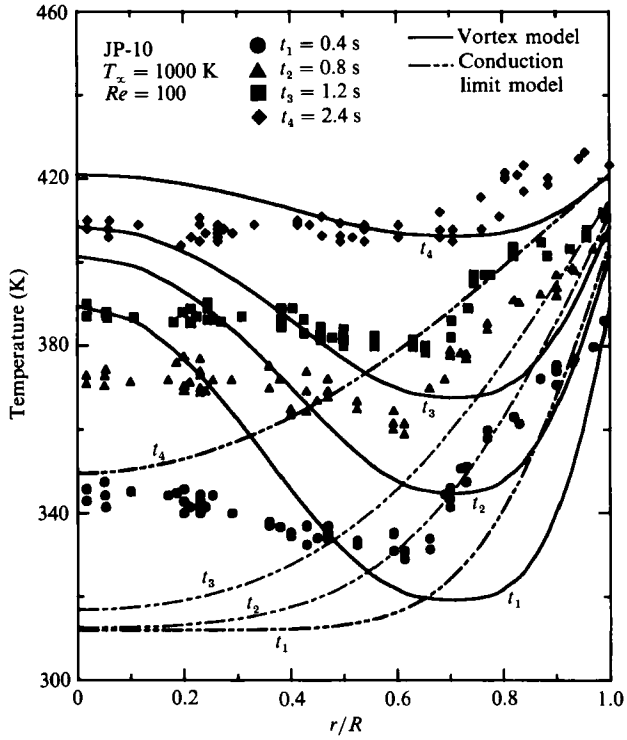

FIGURE 4. Comparison of experimental and theoretical results of droplet temperature distribution at $Re_0 = 100$.

(figure 4). Also compared are the CLM results. The CLM results unsurprisingly differ greatly from the experimental data because CLM is only suitable for $Re \ll 1$. It is, however, very interesting to find that the VM results also differ significantly from the experimental data although they are qualitatively similar. Interesting points related here are: (i) the experimental minimum temperature occurs at $r/R = 0.6$–0.7, slightly differing from the position of $r/R = 0.707$ in the VM results (i.e. the position of the Hill vortex centre). It should be mentioned that the magnitude and position of the experimental minimum values may not reflect the actual ones because the vortex centre does not always remain on the plane where the thermocouples are located; (ii) the experimental temperature distributions appear to lie between the VM and CLM predictions, especially in the droplet-core region. This type of radial temperature distribution implies that the temperature *along* a streamline is far from isothermal. Therefore, the assumption of isothermal streamlines adopted in VM by Sirignano and coworkers is probably not realistic; (iii) as far as surface temperature is concerned, VM exhibits good performance; (iv) although the solutions of the full Navier–Stokes equations for the present case are unavailable, it can be found in Patnaik *et al.* (1986) and Dwyer & Sanders (1984) that the isotherm and streamline patterns, during the heating period, are rather different, with the temperatures near the droplet centre being considerably elevated but significantly lower than the surface temperatures. Therefore, the solutions of the full Naviers–Stokes equations appear to agree with present experimental data. This will be discussed further in the following section.

Figure 5 compares the experimental temperature distributions at various Reynolds

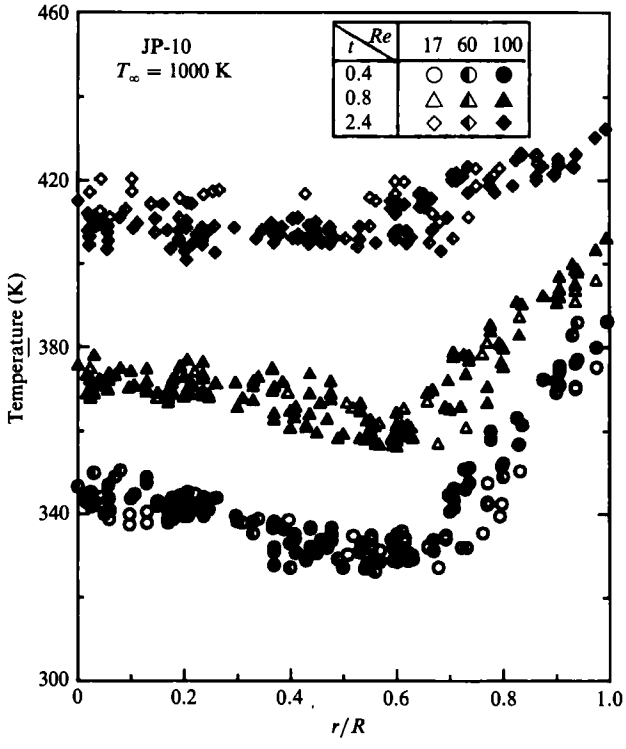

FIGURE 5. Comparison of experimental droplet temperature distributions for $Re_0 = 17$, 60, 100.

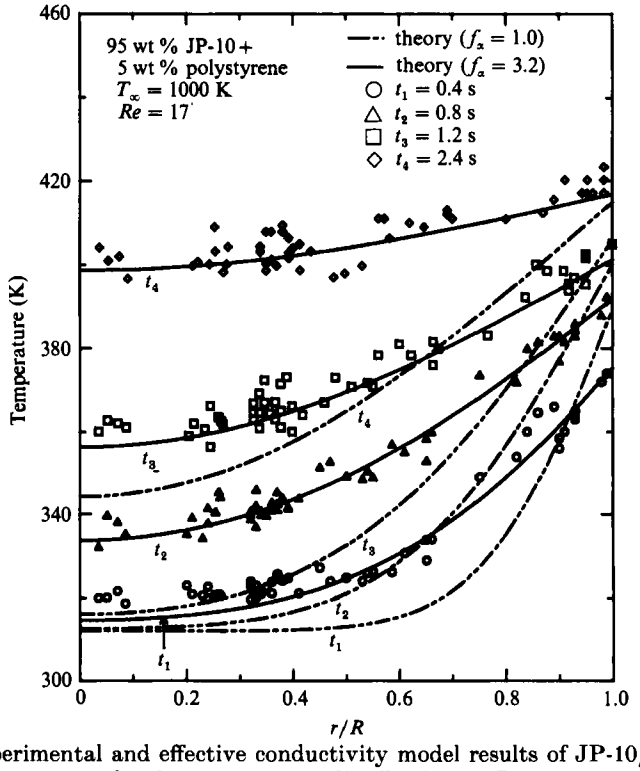

FIGURE 6. Experimental and effective conductivity model results of JP-10/5 wt % polystyrene droplet temperature distribution at $Re_0 = 17$.

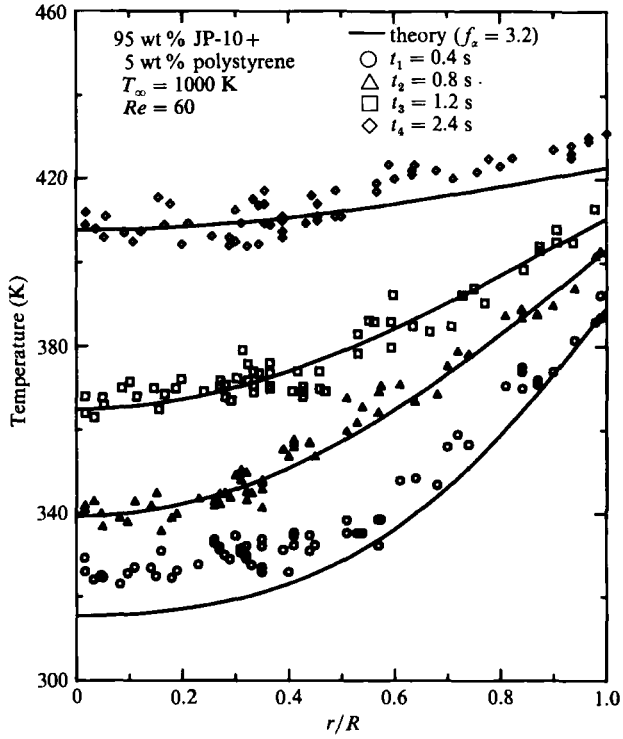

FIGURE 7. Experimental and effective conductivity model results of JP-10/5 wt % polystyrene droplet temperature distribution at $Re_0 = 60$.

numbers ($Re_0 = 17$, 60 and 100). No significant differences can be observed except for a slightly more rapid temperature rise at $Re_0 = 100$. The increased temperature rise rate may be attributed to a higher interfacial convective heat transfer rate occurring at a larger Re. The heat transport mechanism within droplets, as a result, is essentially unvarying at $Re \approx O(10)$–$O(100)$. An increase of Re by a factor of 6 apparently did not substantially enhance internal core motion. In other words, the considerable increase of free-stream momentum failed to have substantial effect across the momentum boundary layers in both phases. Similar results for high-viscosity cases will be shown.

Internal temperature distributions were also measured with liquid viscosity increased. Two main reasons led to this investigation: internal momentum and heat transport mechanisms are essentially related to liquid motion, which is strongly affected by liquid viscosity. More information about internal dynamics and heat transport mechanisms can be obtained from the temperature distribution patterns; no studies concerning effects of liquid viscosity on internal transport mechanisms have been available, although high-viscosity fuels, such as slurry fuels and heavy oils, are important in engineering applications.

High-viscosity fuels were prepared by dissolving 5 or 10 wt % of polystyrene in JP-10. The resultant viscosities were respectively 7.2 and 25 cSt at 100 °C, while the viscosity of JP-10 at 100 °C was 1.15 cSt.

The measured internal temperature distributions of a JP-10/5 wt % polystyrene droplet at $Re_0 = 17$ are shown in figure 6. Interestingly, the temperature decreases monotonically toward the droplet centre. The distribution pattern becomes very

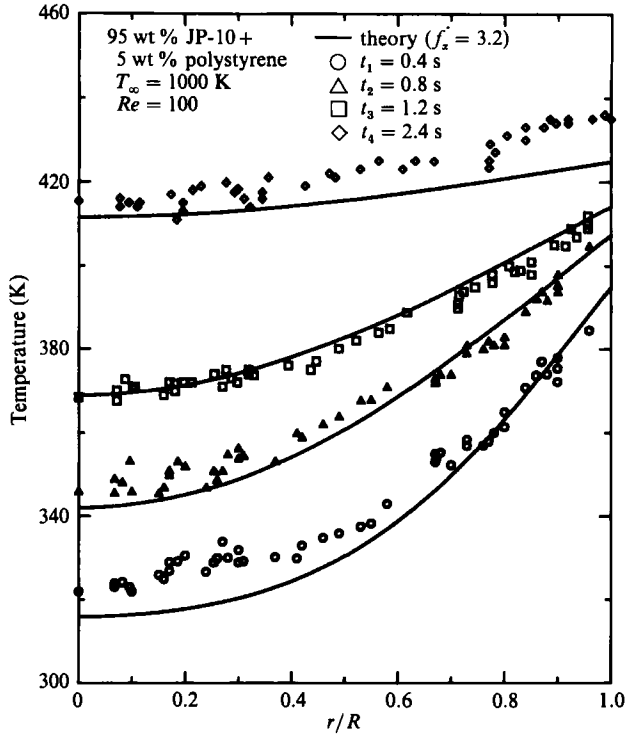

FIGURE 8. Experimental and effective conductivity model results of JP-10/5 wt % polystyrene droplet temperature distribution at $Re_0 = 100$.

different from that of a JP-10 droplet (figure 3*a*), with the vortex model apparently being inapplicable. While the monotonic pattern resembles that predicted by CLM (the $f_\alpha = 1$ curves), the temperature apparently rises more rapidly. The theoretical results of ECM with $f_\alpha = 3.2$ appears to fit the experimental data very well. The calculations excluded the following phenomenon existing in the experiment. The gradually increasing polystyrene concentration led to an increase of viscosity as JP-10 vaporized. The increased viscosity retarded internal circulation and heat transport rates, resulting in slower experimental temperature rises. This, however, is not expected to be significant except at the later stage of heating when a considerable amount of JP-10 has vaporized.

Similar experiments were conducted at higher Reynolds numbers. The results are shown in figure 7 for $Re_0 = 60$ and in figure 8 for $Re_0 = 100$. The best-fit values of f_α remain around $f_\alpha = 3.2$ with an increased Re. A significant increase of Re again failed to effect internal circulation enhancement.

Investigations for a larger liquid viscosity were also conducted. Figure 9 shows the results associated with JP-10/10 wt % polystyrene droplets at $Re_0 = 17$. The best-fit f_α decreases to 2.6, as compared with 3.2 for lower viscosity JP-10/5 wt % polystyrene droplets (cf. figure 6). The internal energy transport rate, again, is found to be related to liquid viscosity, with heat transport being retarded as liquid viscosity increases.

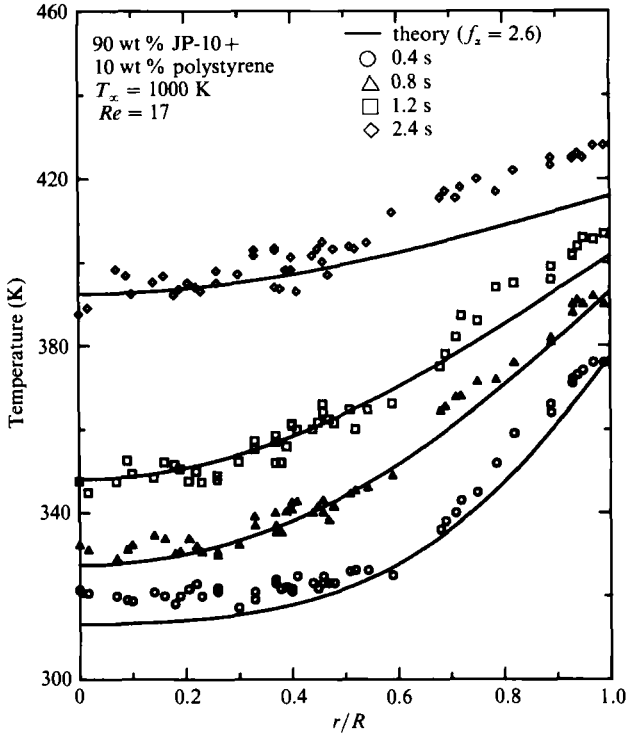

FIGURE 9. Experimental and effective conductivity model results of JP-10/10 wt % polystyrene droplet temperature distribution at $Re_0 = 17$.

4. Discussion

Internal temperature distributions have been carefully measured for various Reynolds numbers and liquid viscosities. These experimental results render important information on the heating mechanisms and internal droplet dynamics.

Figure 4 shows that the vortex model of Sirignano and coworkers is qualitatively correct but quantitatively inaccurate. A key assumption made in VM is: the temperature along a closed streamline is uniform, based on characteristic time analysis for large Reynolds numbers. With this assumption, as well as the internal droplet motion being the inviscid Hill vortex, the formulation could be greatly simplified since heat transfer only exists in the direction normal to the closed streamlines. The assumption of isotherms along streamlines made in VM, however, is not favoured by present experimental data. This assumption was made through the following reasoning (Prakash & Sirignano 1978). (The quantities used here correspond to present experimental conditions.) At an Re as large as $O(100)$, the liquid motion within the droplet is expected to be quasi-steady, consisting of an inviscid Hill vortex in the droplet core and a thin viscous boundary layer near the droplet surface. The Péclet number is $O(1000)$ since the Prandtl number of the liquid is of $O(10)$. The thermal boundary layer near the droplet surface is, therefore, also very thin. The droplet surface velocity, U_s, can be approximately determined using (Law, Prakash & Sirignano 1976)

$$(U_s/U_\infty) \approx (\rho_l \mu_l / \rho_g \mu_g)^{-\frac{1}{3}}. \tag{1}$$

For JP-10 at 100 °C and 1 atm, $\rho_l = 870.5$ kg/m^3 and $\mu_l = 1.0 \times 10^{-3}$ m^2/s; for air at 1000 K and 1 atm, $\rho_g = 0.35$ kg/m^3 and $\mu_g = 4.15 \times 10^{-5}$ m^2/s. So, $U_s/U_\infty \approx 0.03$,

with $U_\infty = 6$ m/s, $U_s \approx 0.2$ m/s. The characteristic circulation time along a closed streamline in the core is

$$\tau_{\text{circulation}} = O(d/U_c),$$

where U_c is the characteristic liquid velocity in the droplet core. Although U_c should be much smaller than U_s, Prakash & Sirignano (1978) inappropriately took U_s as U_c in estimating the circulation time. If Prakash & Sirignano's approach is used, the circulation time is $O(10$ ms) when $d = 2000$ μm. On the other hand, the characteristic thermal diffusion time in the absence of any liquid motion can be calculated as

$$\tau_{\text{thermal diffusion}} = O\left(\frac{(0.3R)^2}{\alpha_l}\right).$$

Let $R = 1000$ μm and $\alpha_l = 4.7 \times 10^{-8}$ m^2/s, the characteristic diffusion time is of $O(2$ s). Since the circulation time thus calculated is smaller than the thermal diffusion time by a factor of $O(\frac{1}{100})$, the assumption of uniform temperature along a closed streamline is valid. However, the characteristic liquid velocity in the core, U_c, should be substantially smaller than the surface velocity, U_s, when considering the existence of the liquid-phase boundary layer. A proper ratio of U_c/U_s, although not directly available, is expected to be of $O(\frac{1}{10})$ to $O(\frac{1}{100})$, according to stream function solutions of the Navier–Stokes equations (LeClair *et al.* 1972; Patnaik *et al.* 1986). If $U_s/U_c \approx O(20)$ is roughly given, the circulation time becomes $O(0.2$ s), which is not negligibly small compared with the thermal diffusion time. Therefore, the assumption of isotherms along the closed streamlines might be inappropriate at $Re \approx O(100)$. Temperature, instead, is likely to continuously decrease along a streamline out of heat dissipation, owing to a significant residence time. This concept is consistent with experimental observations (figures 2–5) as well as temperature solutions of the full Navier–Stokes equations (Patnaik *et al.* 1986). The heat transport mechanism, and hence the temperature distributions, should also be closely related to circulation intensity and liquid viscosity, when Re is less than $O(100)$. The vortex model is satisfactory in the determination of surface temperatures for $Re \approx O(100)$, although it seems to overestimate internal transport (figure 4).

The effects of liquid viscosity on internal temperature distribution can be found by comparing figures 3(*a*), 6 and 9 ($Re_0 = 17$) or figures 4 and 8 ($Re_0 = 100$). A larger liquid viscosity makes a smaller circulation intensity at an identical Re_0. Temperature distributions clearly are influenced strongly by liquid viscosity (or circulation intensity) (figures 3*a*, 6 and 9). For the case of JP-10 ($\nu = 1.15$ cSt at 100 °C), the temperature elevation near the droplet centre manifests significant heat transport through internal circulation (figure 3*a*). The droplet core temperature elevation disappears with increasing viscosity ($\nu = 7.2$ cSt at 100 °C), as in figure 6. This change reflects that less heat is transported into the droplet interior through circulation with a smaller liquid velocity. Significant enhancement of heat transport by internal circulation, however, is still manifested with a larger-than-unity effective conductivity factor ($f_\alpha = 3.2$). If the effective conductivity factor of 3.2 is considered to consist of a diffusive portion of 1 and a circulative portion of 2.2, the relative contribution of circulative transport is somewhat larger than the diffusive contribution. When liquid viscosity further increases ($\nu = 25$ cSt at 100 °C), f_α decreases to 2.6, reflecting a reduced fraction of circulative heat transfer. Similar results concerning liquid viscosity effects can be obtained by comparing figures 4 and 8. Internal temperature distributions and heat transport mechanisms, based on the above experimental results, appear strongly affected by liquid viscosity – even at

$Re_0 = 100$. Consequently, the assumption in VM that the internal temperature distribution is independent of liquid viscosity at Reynolds numbers of $O(100)$ is not favoured by the present experimental results. It is, however, very interesting that the model based on the full Navier–Stokes equations (Patnaik *et al.* 1986) exhibits more consistency with experimental temperature distributions, although it has been shown to suffer an error in drag coefficient prediction (Dwyer 1989). More work is needed in evaluating the reliability of such an approach since the comparison is still crude.

5. Conclusions

1. Transient internal temperature distributions were obtained experimentally for droplets vaporizing in hot gases at initial Reynolds numbers of 17, 60 or 100. Axisymmetric internal vortex motion was clearly demonstrated by the elevated-in-droplet-core temperature distributions for low-viscosity hydrocarbon fuels. This type of temperature distribution also indicated that internal heat transport was significantly enhanced by internal circulation.

2. The vortex model proposed by Sirignano and coworkers (Prakash & Sirignano 1978; Tong & Sirignano 1983; Abramzon & Sirignano 1989) is qualitatively correct, but quantitatively over-predicts internal temperature distributions at $Re \approx O(100)$; this is because they over-estimated the internal liquid velocity. The key assumption of isothermal streamlines adopted in the vortex model is not favoured by experimental evidences. The vortex model exhibits good performance as far as surface temperature is concerned. On the other hand, preliminary examinations revealed that the model which solved the full Navier–Stokes equations (Patnaik *et al.* 1986) probably agrees better with experimental data.

3. A considerable range of Reynolds numbers was not observed to influence temperature distributions for both low- and high-liquid-viscosity cases. This is presumably because the increase of free-stream velocity failed to effect significant core motion enhancement across boundary layers.

4. Circulative heat transport is closely related to liquid viscosity (or circulation intensity). The circulative heat transport progressively decreases as liquid viscosity increases, as indicated by the temperature distributions in which temperature monotonically decreases toward the droplet centre. These temperature distributions could be satisfactorily simulated using the semi-empirical effective conductivity model. Effective conductivity factors, representing a combinatory coefficient of the diffusive and circulative heat transport rate, decreased with respect to a liquid viscosity increase.

The authors gratefully acknowledge the financial support of National Science Council, ROC under Contract no. NSC81-0401-E007-07.

Appendix

Three theoretical models are adopted in this paper for the description of droplet heating processes, with basic differences in liquid-phase analyses. They are the conduction limit model (CLM), the vortex model (VM), and the effective conductivity model (ECM).

A.1. *Liquid phase analysis*

A.1.1. *Conduction limit model*

This model assumes that heat transfer within the droplet is solely by thermal conduction and that the surface temperature is uniform. The conservation equations of mass and energy are

$$\frac{\mathrm{d}m}{\mathrm{d}t} = -\dot{m}, \tag{A 1}$$

$$\frac{\partial T}{\partial t} = \frac{\alpha_1}{r^2}\frac{\partial}{\partial r}\left(r^2\frac{\partial T}{\partial r}\right). \tag{A 2}$$

The initial and boundary conditions are

$$T(r, 0) = T(r), \tag{A 3a}$$

$$\dot{q} = \dot{m}L + 4\pi R^2 k_1 \left.\frac{\partial T}{\partial r}\right|_{r=R}, \tag{A 3b}$$

$$\left.\frac{\partial T}{\partial r}\right|_{r=0} = 0. \tag{A 3c}$$

A.1.2. *Vortex model*

Liquid circulation caused by surface friction was expected to prevail within a droplet subjected to a gas flow. At large Reynolds numbers it has been theoretically found that a thin viscous boundary layer exists near the droplet surface, with droplet-core motion away from the boundary layer being essentially inviscid (Batchelor 1956; LeClair *et al.* 1972; Rivkind *et al.* 1976). Numerical solutions of the Navier–Stokes equations have shown, for a wide range of conditions (Reynolds numbers, ratios of fluid viscosities and densities), the internal streamline patterns are insensitive to internal Reynolds number, resembling very closely an inviscid pattern, known as the Hill vortex (Rivkind *et al.* 1976). Prakash & Sirignano (1978) subsequently developed a model by assuming that the internal velocity field in the droplet is represented by the Hill vortex; and the isotherms inside the droplet coincide with the streamlines, owing to a high liquid Péclet number. Tong & Sirignano (1983) further arrived at a simplified theory with close approximation, referred to as the vortex model in this paper.

A.1.3. *Effective conductivity model*

An alternative approach has been suggested (Talley & Yao 1986; Abramzon & Sirignano 1989) for avoiding the lengthy calculation associated with the vortex model. This approach takes circulative transport enhancement into account by imposing an 'effective' value of the thermal conductivity coefficient to the conduction limit model. This simplified model has been found to possibly fit the vortex model results well when an appropriate factor f_α is used. The mathematical formulation of this model is similar to that of CLM, except for the presence of f_α in heat conduction terms, i.e.

$$\frac{\partial T}{\partial t} = \frac{f_\alpha \alpha_1}{r^2}\frac{\partial}{\partial r}\left(r^2\frac{\partial T}{\partial r}\right), \tag{A 4a}$$

$$\dot{q} = \dot{m}L + 4\pi R^2 k_1 f_\alpha \left.\frac{\partial T}{\partial r}\right|_{r=R}. \tag{A 4b}$$

This model reduces to CLM when $f_\alpha = 1$.

A.2. *Gas phase analysis*

The gas phase will be treated in a simple manner since it is not the focus here. The gas phase analysis has been unified in this paper as follows. The conventional assumption of a quasi-steady gas phase is employed. Following Faeth's approach (1977) to droplet evaporation, the conservation equations of mass, species and energy are

$$4\pi\rho_g v r^2 = \dot{m}, \tag{A 5}$$

$$\frac{\mathrm{d}}{\mathrm{d}r}\left[r^2\left(\rho_g v Y_f - \rho_g D\frac{\mathrm{d}Y_f}{\mathrm{d}r}\right)\right] = 0, \tag{A 6}$$

$$\frac{\mathrm{d}}{\mathrm{d}r}\left[r^2\left(\rho_g v C_{pg}(T-T_\infty) - k_g\frac{\partial T}{\partial r}\right)\right] = 0. \tag{A 7}$$

The boundary conditions are

$$r = R; \quad T = T_s, \quad Y_f = Y_{fs},$$
$$r = \infty; \quad T = T_\infty, \quad Y_f = 0.$$

The mass and heat transfer at the droplet–gas interface are evaluated by

$$\dot{m} = 2\pi R\rho_g D_g Sh \ln(1+B_y), \tag{A 8}$$

$$\dot{q} = 2\pi R k_g Nu(T_\infty - T_s)\ln(1+B_y)/B_y, \tag{A 9}$$

where

$$Nu(\text{or } Sh)(1+B')^{0.7} = 2+0.57Re^{0.5}(Pr \text{ or } Sc)^{0.333}, \tag{A 10}$$

$$B_y = Y_{fs}/(1-Y_{fs}).$$

In (A 10), which is the modified Renksizbulut–Yuen correlation (Dwyer 1989),

$$B' = (C_{pg}(T_\infty - T_s)/L)(1-\dot{q}_l/\dot{q}), \tag{A 11}$$

where $\dot{q}_l$ is the liquid part of the heating,

$$\dot{q}_l = 4\pi R^2 k_l f_\alpha \left.\frac{\partial T}{\partial r}\right|_{r=R}.$$

Thermodynamic properties of JP-10 can be found in Wong & Turns (1987).

REFERENCES

Abramzon, B. & Sirignano, W. A. 1989 Droplet vaporization model for spray combustion calculation. *Intl J. Heat Mass Transfer* **32**, 1605–1618.

Antaki, P. J. & Williams, W. A. 1987 Observations on the combustion of boron slurry droplets in air. *Combust. Flame* **67**, 1–8.

Ayyaswamy, P. S., Sadhal, S. S. & Huang, L. J. 1989 Effect of internal circulation on the transport to a moving liquid drop. *1989 Natl Heat Transfer Conf. HTD*, vol. 107, pp. 131–140.

Batchelor, G. K. 1956 On steady laminar flow with closed streamlines at large Reynolds number. *J. Fluid Mech.* **1**, 177–190.

Dwyer, H. A. 1989 Calculations of droplet dynamics in high temperature environments. *Prog. Energy Combust. Sci.* **15**, 131–158.

Dwyer, H. A. & Sanders, B., R. 1984 Detailed computation of unsteady droplet dynamics. *20th Symp. (Intl) on Combust.* pp. 1743–1749. The Combustion Institute.

Faeth, G. M. 1977 Current status of droplet and liquid combustion. *Prog. Energy Combust. Sci.* **3**, 191–224.

GOGOS, G. & AYYASWAMY, P. A. 1988 A model for the evaporation of a slowly moving droplet. *Combust. Flame* **74**, 111–129.

LAW, C. K. 1982 Recent advances in droplet vaporization and combustion. *Prog. Energy Combust. Sci.* **8**, 171–201.

LAW, C. K., PRAKASH, S. & SIRIGNANO, W. A. 1976 Theory of convective, transient, multicomponent droplet vaporization. *16th Symp. (Intl) on Combust.* pp. 605–617. The Combustion Institute.

LECLAIR, B. P., HAMIELEC, A. E., PRUPPACHER, H. R. & HALL, W. D. 1972 A theoretical and experimental study of the internal circulation in water drops falling at terminal velocity in air. *J. Atmos. Sci.* **29**, 728–740.

PATNAIK, G., SIRIGNANO, W. A., DWYER, H. A. & SANDERS, B. S. 1986 A numerical technique for the solution of a vaporizing fuel droplet. *Prog. Aeronaut. Astronaut.* **105** (II), 253–266.

PRAKASH, S. & SIRIGNANO, W. A. 1978 Liquid fuel droplet heating with internal circulation. *Intl J. Heat Mass Transfer* **21**, 885–895.

RENKSIZBULUT, M. & YUEN, M. C. 1983 Numerical study of droplet evaporation in a high-temperature stream. *J. Heat Transfer* **105**, 389–397.

RIVKIND, V. IA., RYSKIN, G. M. & FISHBEIN, G. A. 1976 Flow around a spherical drop at intermediate Reynolds numbers. *Z. angew. Math. Mech.* **40**, 687–691.

SCHLICHTING, H. 1979 *Boundary Layer Theory*, 7th edn, p. 31. McGraw-Hill.

TALLEY, D. G. & YAO, S. C. 1986 A semi-empirical approach to thermal and composition transients inside vaporizing fuel droplets. *21st Symp. (Intl) on Combust.* pp. 609–616. The Combustion Institute.

TONG, A. Y. & SIRIGNANO, W. A. 1983 Analysis of vaporizing droplet with slip, internal circulation, and unsteady liquid-phase quasi-steady gas-phase heat transfer. *ASME/JSME Thermal Engng Joint Conf. Proc.* vol. 2, pp. 481–487.

WONG, S.-C., LIN, A.-C. & CHI, H.-Y. 1991 Effects of surfactant on the evaporation, shell formation and disruptive behavior of slurry droplets. *23rd Symp. (Intl) on Combust.* pp. 1391–1397. The Combustion Institute.

WONG, S.-C. & TURNS, S. R. 1987 Ignition of aluminum slurry droplets. *Combust. Sci. Tech.* **52**, 221–242.